Polymer Vol. 37 No. 16, pp. 3543–3552, 1996

0032-3861/96/$15.00 + 0.00

S0032-3861(96)00165-6

The influence of starch molecular mass on the properties of extruded thermoplastic starch

J. J. G. van Soest*, K. Benes and D. de Wit
ATO-DLO, PO Box 17, 6700 AA Wageningen, The Netherlands

and J. F. G. Vliegenthart
Department of Bio-organic Chemistry, Bijvoet Center, Utrecht University, PO Box 80.075, 3508 TB Utrecht, The Netherlands
(Received 6 September 1995; revised 20 December 1995)

The mechanical properties of a low and a high molecular mass thermoplastic starch (TPS) were monitored at water contents in the range of 5–30% (w/w). The granular starches were plasticized by extrusion processing with glycerol and water. The low molecular mass starch was prepared by partial acid hydrolysis of potato starch. The extruded TPS materials were stored at 60% relative humidity for 12 months to level out differences in starch structure due to retrogradation. The water content was then varied by an additional storage period at various humidities. The average molecular masses of the TPS materials, composed of native starch or of hydrolysed starch, were 37 000 and 1900 kg mol^{-1}, respectively. The apparent amylose contents of the high and low molecular mass materials were 25% and 11%, respectively. Differences were observed in thermal properties and crystallinity between the two types of materials, as a function of water content but not as a function of molecular mass. The stress–strain properties of the materials were dependent on the water content. The materials showed a viscoelastic behaviour characteristic of a semicrystalline polymer. Materials containing less than 9% water were glassy with an elastic modulus between 400 and 1000 MPa. For the materials a transition from brittle to ductile behaviour occurred at a water content in the range of 9–10%, which is in accordance with the observed glass transition temperature at this water content. The rubbery materials, with a water content of 9–15%, were tough and an optimum in ultimate elongation was observed. Above a water content of 15% the materials became weak and soft and the strain at break decreased. No significant differences in brittle-to-ductile transition as a function of water content were observed between the low and high molecular mass TPS materials. In the rubbery state with 14% water, the elongations at break of the high and low molecular mass materials were 100–125% and 30–50%, respectively. The tearing energy of the materials showed a maximum at a water content of 9–10%. The energies at this maximum of the high and low molecular mass materials were 0.15 and 0.1 J mm^{-2}, respectively. The lower strain and tearing energy of the low molecular mass materials in the rubbery state were attributed to the reduced amylose chain length as well as the molecular mass and the degree of branching of the amylopectin molecules. This resulted in a material with a less effective entangled starch matrix. The entanglements were described as a complex network of the linear amylose chains and the outer chains of the amylopectin molecules in which hydrogen bonding plays an important role. Copyright © 1996 Elsevier Science Ltd.

(Keywords: molecular mass; thermoplastic starch; extrusion)

INTRODUCTION

Over the past decades several efforts have been made to convert starch into a thermoplastic starch (TPS) material. Because of the price, excellent biodegradability and availability from renewable resources[1–5], plastic starch materials are being made suitable for single use biodegradable plastic items such as planting pots, trash bags, shopping bags, and dinner utensils[6–8]. It has been demonstrated that starch can be shaped into moulded articles using standard thermoplastic processing equipment[9–12].

Starch consists of two high molecular mass, polydisperse polymers. Both amylose and amylopectin are α-(1 → 4)-D-glucans, but amyloses are almost linear and amylopectins are highly branched through α-(1 → 6)-linkages occurring every 18–25 residues[13]. Potato starch contains 20–30% amylose[14,15]. Amylose molecular masses range from 10^1 to 10^2 kg mol^{-1}, while amylopectin molecular masses are in the range of 10^4–10^6 kg mol^{-1}[16,17]. Starch molecular mass and amylose/amylopectin ratio in TPS are not only dependent on starch source but also influenced by processing conditions, such as temperature and shear, and by type of processing, such as extrusion, kneading, pressure and injection moulding. Several studies have been published

* To whom correspondence should be addressed

on the influence of molecular mass of starch on the gelation properties of several starches and on the mechanical properties of starch cast films from modified starches[18 23]. However, no data are available concerning the relationship between the molecular mass of the starch polymers and the mechanical properties of extruded TPS materials. Changes in molecular mass and plasticizer content have been shown to affect the mechanical properties of petrochemical thermoplastics[24]. One of the most important parameters determining the properties of thermoplastic materials is the glass transition temperature (T_g). The T_g of starch is determined by plasticizer type and level[25-27]. Water and glycerol are the most commonly used plasticizers in amylose or starch casting films and during extrusion, kneading, pressure and injection moulding of TPS[28-32]. Water is probably the most important component giving rise to changes in the properties of TPS materials. However, limited information exists about the influence of water content on the morphology, starch structure, and thermal properties in relation with the mechanical properties of extruded or moulded TPS materials[33 35].

The purpose of this work is to develop an understanding of the influence of starch structure and amylose and amylopectin molecular mass on the mechanical properties of TPS. The properties of a low and a high molecular mass starch are investigated in relationship with water content. The TPS materials are made by extrusion processing of granular potato starch and partial acid hydrolysed potato starch. The materials are stored above T_g for a long period to eliminate differences in starch structure due to differences in retrogradation kinetics. An additional period of storage at various humidities is applied to obtain variations in water content. The differences in morphology, starch structure and thermal properties, as a result of the variations in water content, molecular mass and amylose/amylopectin ratio are related to the stress–strain behaviour of the TPS materials.

EXPERIMENTAL

Materials

Potato starch (PN, potato starch native) and potato starch amylose were obtained from Avebe, Foxhol, The Netherlands. Hydrolysed starches were prepared by suspending granular potato starch in 0.25 M (PH) or 1 M (Ph) hydrochloric acid (25% w/w). The suspension was stirred for 1 h at 23°C, then filtered over a porous glass filter (G3, 16–40 μm) and washed several times with deionized water until a pH of 6.5–7 was reached, then dried for 2 days at 40°C. The water content of the starches was 18%.

L-α-lysophosphatidylcholine (LPC) from egg yolk (L-4129) was from Sigma Chemical Co., St. Louis, USA.

Extrusion

TPS samples were prepared by extruding narrow sheets using a Haake Rheocord 90 system equipped with a laboratory-scale counter-rotating twin screw extruder fitted with a slit die. The die had a width of 25 mm and a height of 0.3 mm. The starches were premixed with glycerol to give the following composition: starch : water : glycerol = 100 : 21 : 30. The mixtures were manually fed into the extruder. The torque was held constant at 55 ± 10 N m. The screw rotation speed was 50 rpm. The temperature profile along the extruder barrel was 80, 135, 120, 90–100°C (from feed zone to die). The melt temperature in zone two was 120°C. The die melt temperature was kept below 100°C to prevent the melt from boiling and to give a bubble-free extrudate.

Storage conditions

Part of the extruded product was stored at −22°C after quenching (rapid cooling in liquid nitrogen) of the hot polymer melt directly after extrusion below T_g. The rest of the extruded ribbons were cut into tensile bars and stored above T_g at 60% relative humidity (RH) and 20°C for 12 months (aging period). After this initial storage period, variations in water content of the materials were achieved by conditioning in desiccators at controlled humidities of 0–90% RH for a period of 1 week. The controlled humidities were obtained by standard salt solutions[36].

Moisture determination

Because of the tendency of TPS to adsorb or desorb water, special care was taken to measure the water content at the time of testing. The samples were milled under cryogen conditions. The water content of the powder (1 g, size <125 μm) was determined gravimetrically either with an infra-red dryer (Sartorius MA40) at 95°C or with a Gallenkamp vacuum oven, at 70°C and a pressure of less than 100 mBar overnight. In view of the volatility of glycerol, the measurements with the infra-red dryer did not exceed 5 min to minimize the loss of glycerol.

Mechanical testing

Dumb-bell specimens according to the ISO 1184-1983 (E) standard were cut from the extruded ribbons directly after extrusion and stored. The sheet thickness varied and so sample dimensions were not identical. Corrections for these differences in thickness were made before measurements. A Model 4301 Instron Universal Testing Machine was operated at a grip length of 80 mm and a crosshead speed of 10 mm min^{-1}. For each variation in water content, two to eight tensile bars were tested at 20°C and 60% RH. The tensile stress at maximal load was calculated on the basis of the original cross-sectional area of the test specimen by the equation: $\sigma = F/A$, wherein σ is the tensile stress, F is the force and A is the initial cross-sectional area. The percentage strain or elongation was calculated on the basis of the length of the narrow parallel portion, by the formula: $(l - l_1)/l_1 \times 100\%$, wherein l is the distance between the gauge marks (in mm) and l_1 is length of the narrow parallel portion (i.e. 33 mm), which is related to the original gauge length by $l_0/l_1 = 25/33$. The elastic modulus (E-modulus) was calculated from the initial slope of the stress–strain curve. The energy to break point, i.e. tearing energy (J mm^{-2}), was measured as the area under the stress–strain curve divided by the area of the transverse section of the samples.

Molecular mass determination

Molecular masses were determined with a HPSEC-MALLS-RI (high performance size exclusion chromatography with a multi-angle laser light scattering detector and a differential refractometer)[37]. The starches

were dissolved in 1 M sodium hydroxide (4 mg ml^{-1}) by stirring for 15–20 h. The sample was filtered over a PTFE filter (1 μm) and injected into a sample loop (200 μl). The sample with eluent, 0.025 M sodium hydroxide, was pumped (Waters Model 6000A solvent delivery system) into a guard column (TSK PWH-PRE prep-guard, 7.5 × 7.5 mm, Beckman) followed by six main columns (Spherogel^{TM}-TSK 1000PW, 2000PW, 3000PW, 5000PW, 5000PWHR and 6000PW, 30 × 7.2 mm, Beckman). The eluate was first examined with a Dawn-F multi-angle laser photometer (Wyatt Technology Inc., Santa Barbara, USA), with an argon-ion laser operating at 488 nm and equipped with 15 detectors in the angular range of 15–151°. Absolute calibration of the photometer was performed with toluene (Uvasol quality, Merck; filtered over a 0.2 μm Acrodisc filter, Gelman) with a Raleigh ratio of 3.975×10^{-5} cm^{-1}. Normalization of the photodiode detectors was performed with Dextran T-500 (Pharmacia) with a radius of gyration of 17 nm. Subsequently, the eluate was examined (on-line) by a RI detector (Waters 410 differential refractometer). The total system was held at a constant temperature of 50°C. The responses from the detectors were transmitted to a personal computer for data analysis.

The results measured by means of the laser light scattering were analysed by the ASTRA 2.04 and EASI 6 Wyatt Technology software. The molecular masses were calculated according to the dn/dc method (with a refractive index increment, dn/dc, of 0.145 ml g^{-1} [38]) with a fifth order polynomial fit. The molecular mass distribution (*MWD*), the number-average ($\bar{M}_n$), the mass average ($\bar{M}_w$), and the z-average ($\bar{M}_z$) molecular masses were calculated from the raw and extrapolated data with the EASI 6 software. Extrapolation was done for the low molecular mass part of the chromatograms on the basis of a calibration curve of dextrans, maltooligosaccharides, maltose and glucose with molecular masses in the range of 25 000 to 0.18 kg mol^{-1}.

Differential scanning calorimetry

Differential scanning calorimetry (d.s.c.) measurements were performed with a Perkin-Elmer DSC-7. Calibration was done with indium (ΔH_{fusion} = 28.59 J g^{-1}, melting point (T_{onset}) = 156.60°C) and Gallium (ΔH_{fusion} = 79.91 J g^{-1}, melting point (T_{onset}) = 29.78°C). An empty pan was used as a reference. Samples were weighed accurately into stainless steel pans and sealed hermetically. For obtaining the melting profile, samples of 30–40 mg were heated from 20 to 230°C at a rate of 10°C min^{-1}. The T_gs were determined by heating the samples (30–40 mg) from 20 to 150°C at a rate of 10°C min^{-1}, followed by cooling down to −50°C at a rate of 200°C min^{-1} and rescanned at a rate of 20°C min^{-1} to 200°C.

Determination of the amylose content was performed on the basis of the melting enthalpy of the amylose-LPC complex[14,15]. 50 μl LPC solution (3% w/v in water) was added to the starch samples (10 mg) in the d.s.c. pans. The samples were heated from 20 to 140°C at a rate of 10°C min^{-1}, then cooled to 20°C at a rate of 200°C min^{-1}, stabilized for 2 min at 20°C and reheated to 140°C at a rate of 10°C min^{-1}. The amylose content was calculated on the basis of dry starch material with the following relation: (% amylose) = $(\Delta H_m)/(\Delta H_c) \times 100\%$, wherein ΔH_m is the measured enthalpy of the melting transition of the LPC-amylose complex in the second scan and ΔH_c is the enthalpy of the pure potato amylose complex with LPC (22.1 J g^{-1}). The potato starch amylose was essentially free of amylopectin (<0.5%) with an average molecular mass of 400 ± 200 kg mol^{-1} as determined with light scattering.

Morphology

The amount of residual granular structure was determined with polarization microscopy. The sliced materials were viewed at a magnification of 40× with a Axioplan Universal Microscope. Photographs were taken using the MC100 camera accessory. Density measurements were made by suspending about 10 g of material in paraffin oil (OPG-Farma) with a density of 0.875 kg l^{-1} and measuring the amount of displaced paraffin oil.

Fourier transform infra-red spectroscopy

Absorbance spectra were recorded on a BioRad FTS-60A spectrometer using the Digilab attenuated total reflectance accessory with a ZnSe-crystal at an angle of incidence of 45°. Sieved samples (with a particle size below 125 μm) were measured directly. The spectra, obtained at a resolution of 4 cm^{-1}, were averages of 400 scans, and were recorded against an empty cell as background. Spectra were baseline corrected at 1200 and 800 cm^{-1} and deconvoluted using techniques described by Cameron and Moffat[39] with a half-width of 15 cm^{-1} and an enhancement of 1.5 with triangular apodization.

X-ray diffractometry

Wide-angle X-ray diffraction (WAXD) patterns were measured using a Philips powder diffractometer (Model PW3710) operated at the CuKα wavelength of 1.542 Å and at 2000 mW. The scattered radiation was detected using a proportional detector. Measurements of diffracted intensities were made in the angular range of 4–40° (°2θ) at ambient temperature. Crystallinity was measured according to the methods of Hermans and Weidinger[40]. Diffractograms were smoothed (with a six point averaging and a band broadening of 1.4) and baseline corrected by drawing a straight line at an angle of 7°. The height of the crystalline diffraction at an angle of 17.3° (°2θ), H_c, was measured relative to the height of the total diffraction, H_t, measured from the baseline. The ratio $R(X_B) = H_c/H_t$ is related to the relative amount of B-type crystallinity, $\%X_B$, in comparison with granular potato starch ($\%X_B$ of granular potato starch is 100%) by the relation: $\%X_B = \{R(X_B) - 0.095\}/0.0055$. The crystallinity of granular potato starch is estimated as 25%.

RESULTS AND DISCUSSION

Structural characterization of the extruded TPS materials

The degree of gelatinization and granular melting, the morphology and the starch structure have been determined of TPS materials which have been stored below T_g by quenching the hot polymer melt directly after extrusion processing. The density of materials with 10–12% water is 1.46 g cm^{-3} for both PN and PH materials. The density of dry granular potato starch is

1.52 g cm^{-3}. The processing of both materials does not give rise to a difference in the macroscopic density of the PN and PH TPS materials.

A typical chromatogram of the starch PH materials is shown in *Figure 1*. For each slice in the chromatogram, the molecular masses determined on the basis of the light-scattering measurements are included in *Figure 1a*. The combination of the concentration detection and the light scattering signals gives the average molecular masses and the molecular mass distribution (*Figure 1b*). The average molecular masses of the various materials are summarized in *Table 1*, showing that during extrusion a breakdown of the starch has taken place. Obviously, the molecular masses of the PH and Ph materials are lower than those of the PN materials due to the hydrolysis. The fraction of molecular masses below 3 kg mol^{-1} is less than 1%.

Typical d.s.c. thermograms of the melting of the amylose–LPC complexes are given in *Figure 2*, illustrating that the complexation abilities of the PN materials are larger than those of the PH and Ph materials. This indicates a decrease in amylose content due to acid hydrolysis. The change in complexation ability for hydrolysed starch is even more pronounced when treated at higher hydrochloric acid concentrations (*Table 2*). The breakdown of amylose is confirmed by the decrease in

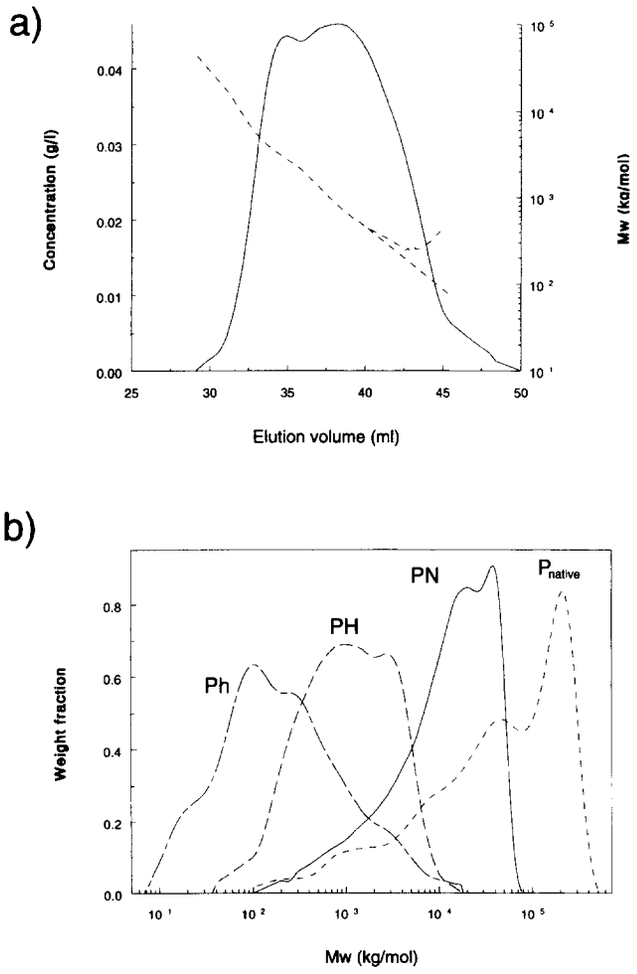

Figure 1 (a) Chromatogram (——) of the extruded PH TPS material with the calculated molecular masses (----). (b) Molecular mass distribution of the extruded Ph, PH and PN TPS materials in comparison with native potato starch (P_{native}), respectively from left to right

Table 1 Molecular masses[a] of granular potato starch and the extruded PN, PH and Ph TPS materials

Material	Average molecular mass (10^{-3} × kg mol^{-1})					
	$\bar{M}_n$	$\bar{M}_w$ Astra	$\bar{M}_z$	$\bar{M}_n$	$\bar{M}_w$ Easi	$\bar{M}_z$
Native	55	99	172	3.5	88	181
	48	96	170	5.4	89	186
PN	26	49	159	1.7	39	190
	23	43	148	1.2	35	178
PH	0.69	1.9	5.2	0.55	1.9	5.3
	0.93	1.8	4.9	0.57	1.8	5.0
Ph	0.4	1.2	6.5	0.2	1.1	6.9
	0.3	1.0	4.1	0.2	0.9	4.3

[a] All samples were measured in duplicate with an accuracy of approximately 10% for $\bar{M}_w$ and 25% for $\bar{M}_n$ and $\bar{M}_z$ values

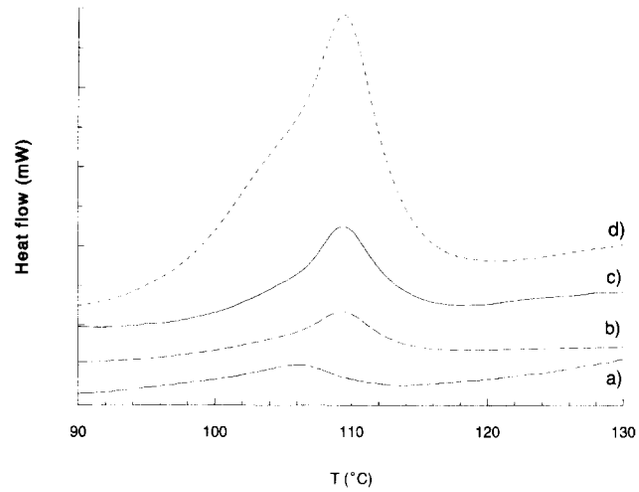

Figure 2 Thermograms of the melting of the amylose-LPC complexes. From bottom to the top are shown: (a) Ph-TPS; (b) PH-TPS; (c) PN-TPS; (d) potato starch amylose

Table 2 Apparent amylose content calculated on the basis of the LPC complexation capacity for native potato starch and the extruded TPS materials

Material	Enthalpy (J g d.s.$^{-1}$)[a]	Amylose (%)	$\bar{M}_w$ (kg mol^{-1})	Preparation method
Potato starch	6.0 ± 0.5	27 ± 3	88 000	native, granular
PN	5.5 ± 0.7	25 ± 3	37 000	native, extruded
PH	2.5 ± 1.0	11 ± 5	1900	hydrolysed (0.25 M), extruded
Ph	1.9 ± 0.4	9 ± 2	1000	hydrolysed (1 M), extruded

[a] d.s., dry starch material

apparent amylose content observed for hydrolysed potato starch (Lintner starch[41]). No significant changes in complexation abilities have been observed between the materials before and after extrusion. The reduction in molecular mass during extrusion processing (*Table 1*) does not lead to a drastic reduction in amylose content. Although a possible breakdown of amylose can take place, the shorter chains are long enough to give a LPC-complex.

With the aid of polarized light microscopy, it is shown that a small amount of granular starch (0–10%) is still present, indicating that not all granular starch is

destructurized. However, no differences are observed for the PN and PH materials.

Some typical thermograms of the premix of PN and the PN TPS material quenched directly after extrusion are shown in *Figure 3a*. Similar melting profiles of the PH premix and the PH TPS materials are observed. The onset melting temperature of the starch–water–glycerol mixture before extrusion is approximately 100°C. The peak temperature is approximately 120°C. The melting temperature during extrusion is only 120°C, with a barrel temperature of 135°C. From a melting point of view, it has to be noted that this can result in some residual, not completely destructurized, granular starch. The process of extrusion is taking place at a high shear stress with a high value of the mechanical energy input which has been shown to enhance melting[46]. Small broad endothermic transitions characteristic of granular melting are observed in the extruded TPS materials. The thermograms measured with an excess of water added show a gelatinization endotherm of some residual granular starch at an onset temperature of 57°C with an enthalpy of 0–1 J g^{-1}. This is indicative of an almost amorphous, completely destructurized TPS starch material, which is in agreement with the low amounts of granular structure determined with polarized light microscopy.

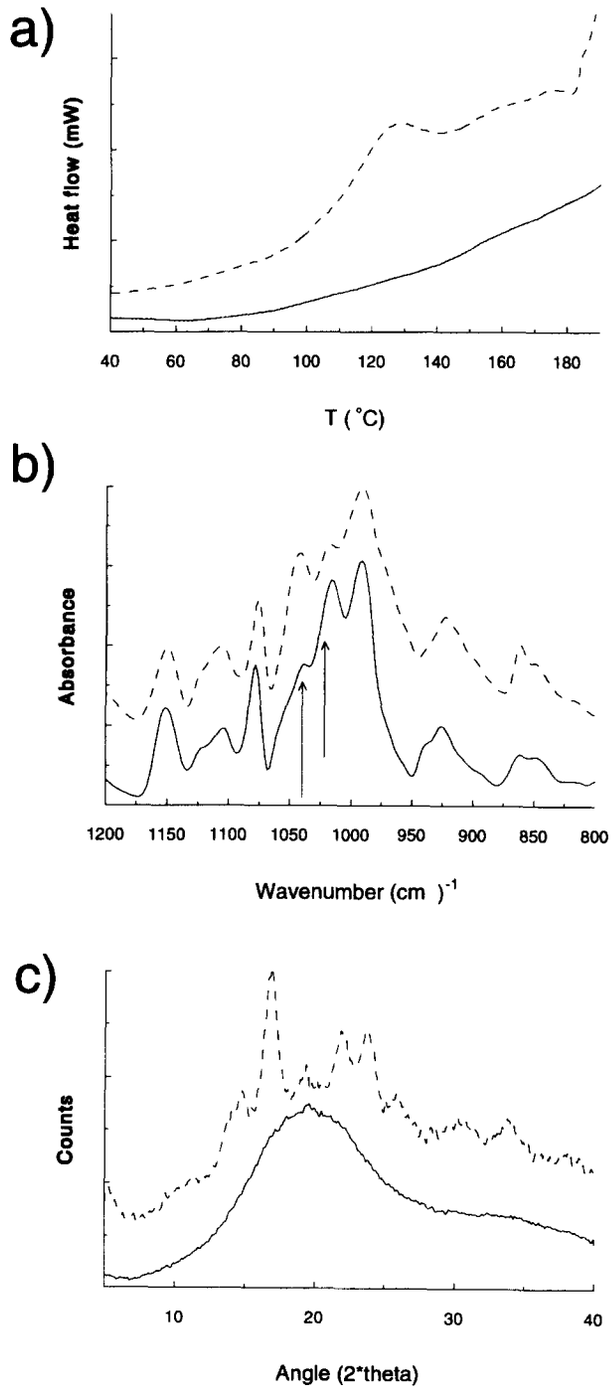

Figure 3 (a) Thermograms of the melting of the premix of granular potato starch (---) and PN TPS stored below glass transition temperature (——). (b) *FT*i.r. spectra of native potato starch (---) and PN TPS stored below T_g (——). (c) X-ray diffractograms of native potato starch (---) and PN TPS stored below T_g (—)

Changes in short-range structure[45] as a result of extrusion are shown in *Figure 3b* for the PN starch premix and the PN TPS materials. The PH materials give similar spectra. The ordering before extrusion processing is high as shown by the high intensity of the band at 1047 cm^{-1} and the low intensity of the band at 1022 cm^{-1}. Extrusion results in a decreased intensity of the band at 1047 cm^{-1} and an increased intensity of the band at 1022 cm^{-1}. The native granular starch is plasticized by extrusion giving a material with low amount of short-range ordering. It is difficult to quantify the amount of ordered structure accurately, because the infra-red (i.r.) spectra are also influenced by slight differences in water and glycerol content.

As shown in *Figure 3c*, the B-type crystallinity observed in granular potato starch is completely destroyed during extrusion. Both the PN and the PH TPS materials are amorphous without any long-range ordering, i.e. amorphous, when stored at low temperature.

Influence of aging and water content on the starch structure in the TPS materials

During storage no changes in birefringence have been observed for either PN or PH materials. Over the whole range of water contents the morphology of the TPS materials shows no differences. Some typical melting profiles of the TPS materials after storage for 12 months are shown in *Figure 4*. Broad double melting endotherms are observed for materials with a water content in the range of 5–30% water. With excess of water added before d.s.c. experiments, less broad melting endotherms are observed at 57°C (onset temperature). The melting above 57°C is due to the melting of some native granular starch or recrystallized starch. The melting of native starch with glycerol added will occur at an onset temperature of 57°C at high water contents. The onset temperature is shifted to 100°C at lower water contents dependent on glycerol content (unpublished results). Another endotherm at 58°C (peak temperature) with an onset temperature of 49°C, is observed in materials which have been stored at low humidities and water contents below 12%. The occurrence of these type of endotherms at 58°C has been explained for several polysaccharides, plasticized with water and stored below or at their T_g, in terms of a dynamic hydration model in which specific energetic water–carbohydrate interactions are involved[42] and by sub-T_g structural relaxation processes involving polymer–polymer interactions[43]. Similar results are obtained for the PH materials. The results are difficult to quantify, because of the low enthalpy changes and the complex nature of the melting profile.

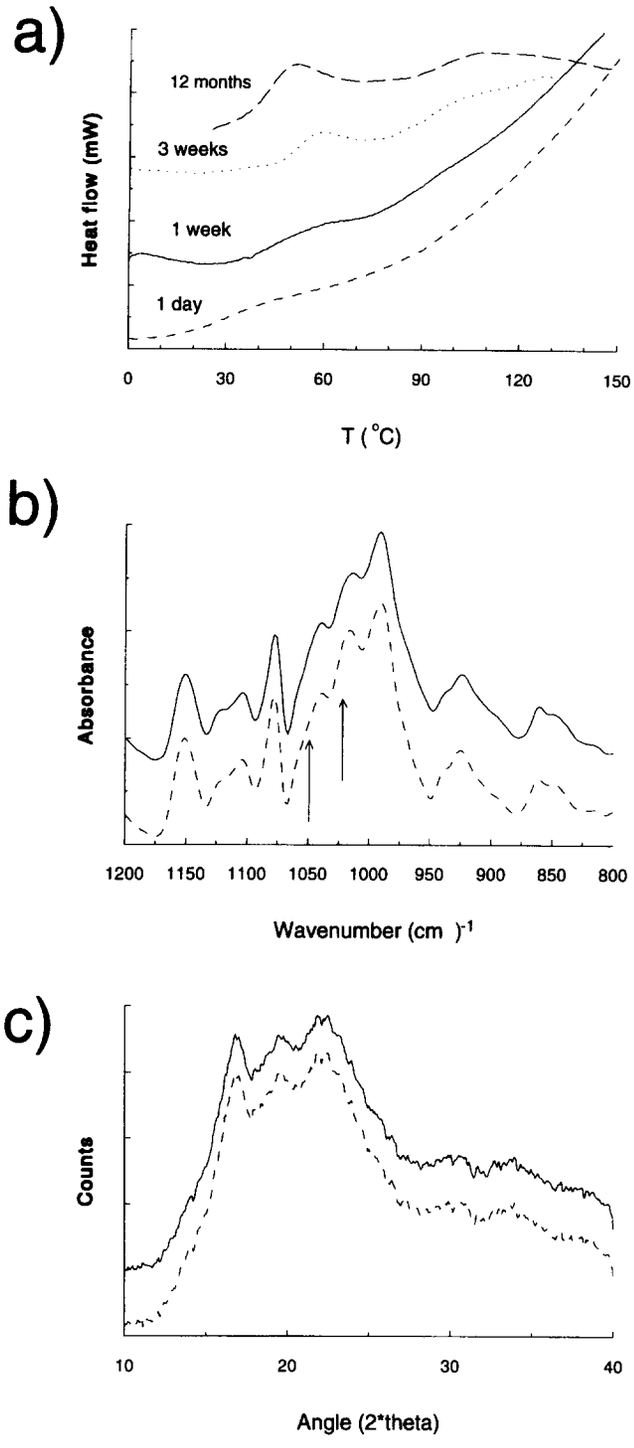

Figure 4 (a) Some typical d.s.c. thermograms of PN TPS materials after aging for various periods as indicated in the figure. (b) *FT*i.r. spectra of PN (——) and PH (- - -) TPS materials. (c) X-ray diffractograms of PN (——) and PH (- - -) TPS materials. The materials have been stored for 12 months above T_g at a RH of 60% and 20°C unless stated otherwise

During storage for 12 months, the amount of crystallinity is increased as shown in *Figure 4b*. Crystallization takes place in materials stored above the T_g of the TPS materials (unpublished results). The water content of the materials stored at 60% RH is 13.5–14.5%. The crystallization process is slow which means that the materials with 13.5–14.5% water are only slightly above their T_g at 20°C. The crystallinity is mainly of the B-type although a small amount of V_h-type structure (unpublished results) is observed for the PN materials. This type of crystal structure is formed solely by amylose and not by amylopectin and the relative abundance is dependent on amylose content which is lower for the PH materials than for the PN materials. The degree of crystallinity of the samples used for mechanical testing of both PN and PH materials amounts to approximately 4.3% irrespective of water content.

The i.r. spectrum of the PN TPS material stored for 12 months is given in *Figure 4c*. The intensities of the bands at 1047 and 1022 cm^{-1} are not changed to a great extent. Thus, the short-range ordering is only slightly increased in time for both the PN and PH materials. The effect of water content on the i.r. spectra of the PN TPS materials is more pronounced. The spectra of the PN TPS materials are similar to those of the PH TPS materials at identical water content. This means that for the materials with the same water content the starch in the material has a similar short-range structure. For materials with low water content (less than 10%) a band broadening is observed in the C–C and C–O stretching region (800–1300 cm^{-1}) due to a lower mobility of the starch chains and ordering of the polymers. The band at 1000–994 cm^{-1} is shown to be related to the C–O–H bending vibrations and is very sensitive to hydrogen bonding[45]. The intensity of the band at 1000–994 cm^{-1} is drastically decreased with increasing water content, from 15 to 30%. The interaction between the starch chains is mainly by hydrogen bridging. Thus, the starch–starch interactions are rapidly decreased at high water content. Also the mobility of glycerol will be increased and the glycerol–starch interactions will be lowered by an increase in water content[47].

Glass transition temperature

A second order phase transition (*Figure 5*), explained as a glass transition, is observed at 30–60°C for brittle materials with 5–10% water. For materials with 11% water the T_g is 20–30°C and for rubbery materials (14% water), it is approximately 0–10°C. For materials with more than 14% water, T_g is difficult to detect. As is shown in *Figure 5*, the T_g far above room temperature is

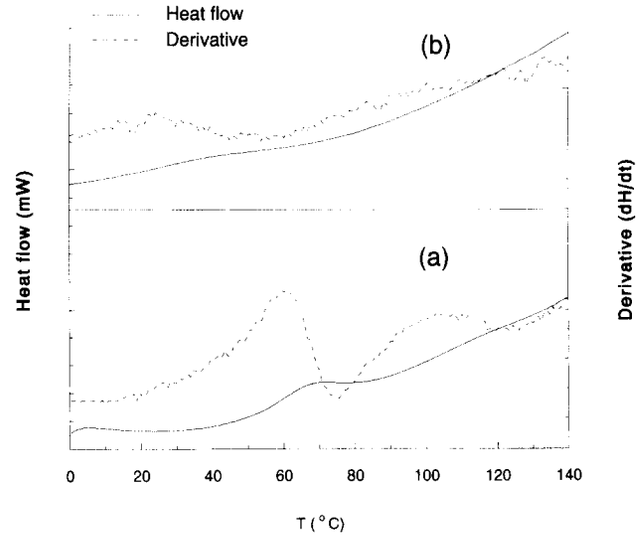

Figure 5 Typical d.s.c. thermograms of the determination of T_g of a PN TPS material with (a) 5% and (b) 11% water

easy to observe, becomes less broad and is often overlapping with the first order sub-T_g transitions described above. The transitions at lower temperatures are very broad ($T_{onset} - T_{conclusion}$ can be up to 30°C) due to the fact that the TPS materials are very complex in compositions. The materials are composed of amylose and amylopectin with a very broad range of molecular masses. As a result T_gs are not detectable for PH materials. No major differences in T_gs are expected on the basis of molecular mass[44]. The results are summarized in *Table 3*.

Mechanical properties: influence water content

Some typical load–strain diagrams of the PN and PH plastics at various water contents are shown in *Figure 6*. The plots are essentially linear at low strains and curve towards the strain axis at higher strains. At water contents less than 5% the materials were too brittle to be measured. Brittle fracture is marked by a rapid decrease in stress at low water content (5–7%). Yielding is not observed because brittle polymer materials break before reaching a yield point. The load–strain curves show a ductile region, with a yield point after which the stress decreases with strain (stress softening) at a water content of 7–10%. The yielding materials are tough. Tearing, a slow fracturing process, is seen at higher water contents. At these water contents no yield point is observed, but the load–strain curve is very smooth with a gradual decrease in stress with strain.

Table 3 Glass transition temperatures

Water content (%)	T_g (°C)[a] PN	PH
20	n.d.	n.d.
14	5	n.d.
11	25	n.d.
8	42	n.d.
5	59	58

[a] Standard deviation is 5°C
n.d., not detectable

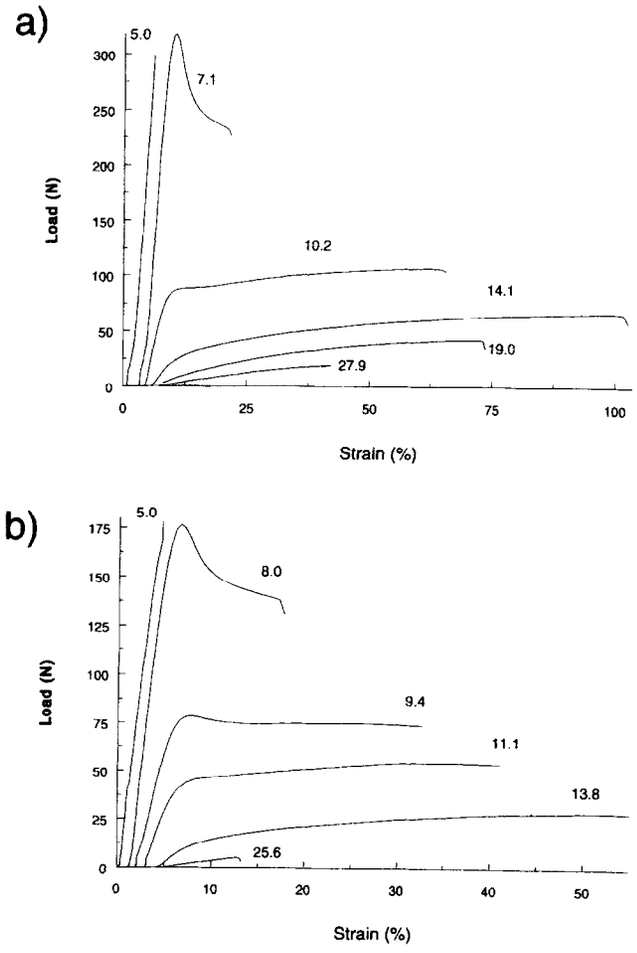

Figure 6 The load–strain diagrams of (a) PN and (b) PH TPS materials at various water contents. The water contents (% w/w) are as indicated in the figure

The E-moduli, derived from the initial slope of the load–strain plots, and the tensile stress at maximal load are shown as a function of water content in *Figures 7a* and *c* and *7b* and *d*, respectively. With increasing water content, a decrease in E-modulus and stress is observed. The E-modulus reaches a value in the order of 500–1000 MPa at low water content (5–7%). The E-modulus drops to a value in the range of 0–100 MPa at a water content of 13–15%. The strain at break vs water content is shown in *Figures 8b* and *d* for both materials. At a water content of 13–15% the materials have a maximum in the elongation at break. Above 15% water the materials become weak and the ultimate elongation is decreased. The energy to break point as a function of water content is shown in *Figures 8a* and *c*. In these curves a maximum is observed at 9–10% water content.

The decrease in E-modulus with increasing water content is characteristic of a polymer being plasticized through its glass-to-rubber transition. At low water content with E-moduli above 500 MPa the material is glassy, and at intermediate water content when the E-moduli are in the range of 10–250 MPa the material is rubbery. The modulus usually drops steeply in the region centred around the glass transition. This change in E-modulus is accompanied by a sharp increase in elongation and tearing energy. The changes in mechanical properties due to a glass-to-rubber transition are in agreement with d.s.c. experiments. For extruded starch materials, with only water added as a plasticizer, a more marked change in properties has been observed in the range of water content of 18–20%[33–35]. This shift of glass-to-rubber transition to a lower water content means that glycerol has a plasticizing effect on the TPS materials, although the effect of glycerol is less than that of water.

Above a water content of 15% the materials are weak and soft, with low elongation and low energy to break point. The materials are not completely elastic but act more like stiff gel-like materials. Permanent deformations up to 30% are observed. This region at high water content is characterized by a loss in properties, i.e. a lower strain, strength and elastic modulus. Water is acting as a plasticizer, lowering the T_g. But at high water content the interactions between starch molecules are weakened to such an extent that the materials become very weak in strength with a low elastic modulus. This weakening of the interactions, especially H-bridges, between the starch molecules is confirmed by i.r. spectroscopy as seen by a reduction of the intensity of the absorbance at 994–1000 cm^{-1}.

Mechanical properties: comparison of the PN and PH materials

The shape of the curves of the tensile stress and elastic

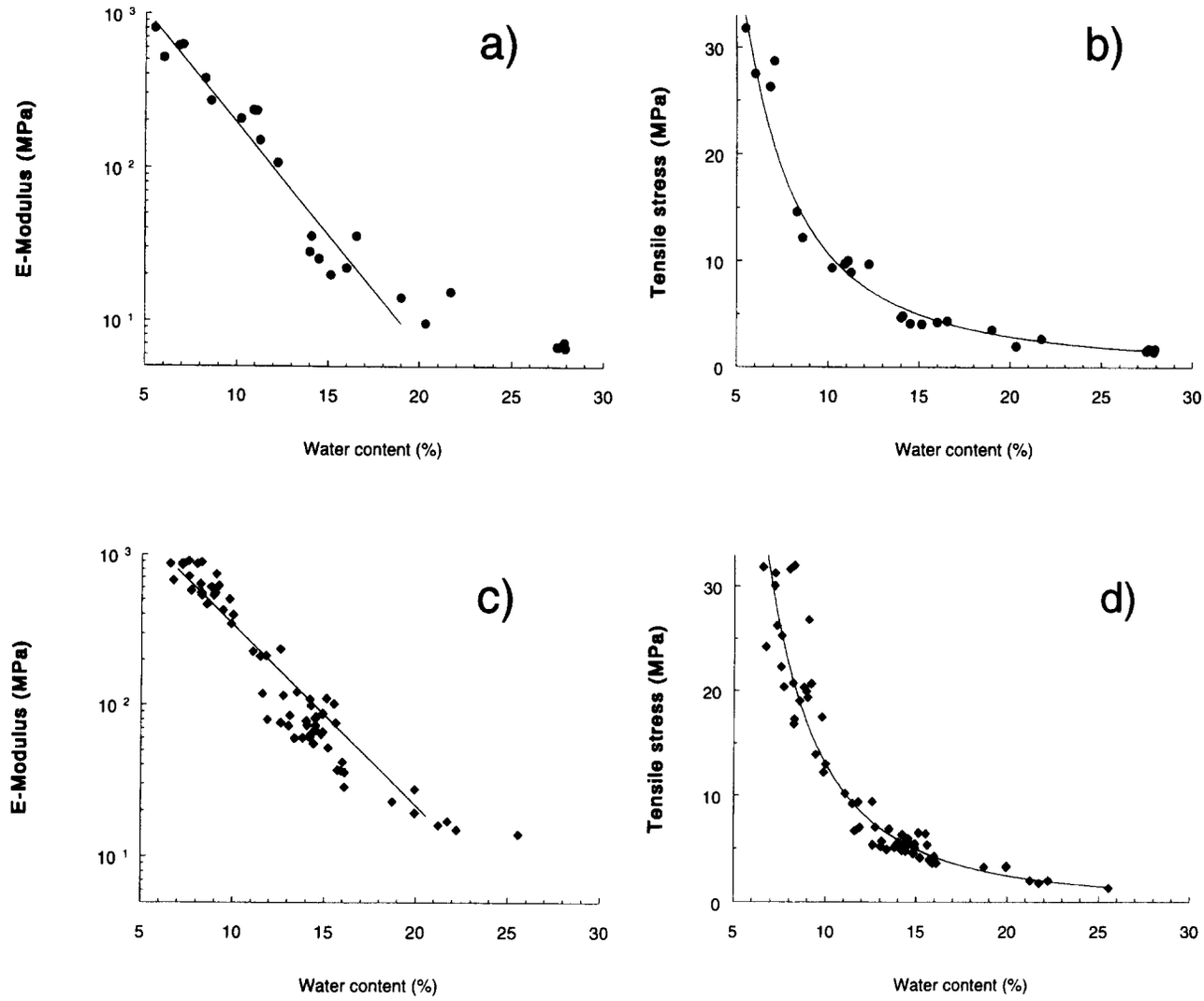

Figure 7 The elastic modulus and tensile stress as a function of water content. ●, E-modulus (a) and tensile stress (b) of the PN TPS materials; ◆, E-modulus (c) and tensile stress (d) of the PH TPS materials

moduli *versus* water content are similar for the PN and PH materials. The changes from glassy to rubbery behaviour occur for both PN and PH materials at the same water content. The differences in molecular mass have no major effect on T_g because the T_g of starch and maltodextrins becomes independent of chain length above 20 glucose units[44]. The change from brittle to ductile behaviour is confirmed by the increasing strain and energy to break point for the PN and PH materials. No differences in E-modulus and glass-to-rubber transition are expected on the basis of the similar morphology, crystallinity and physical structure of the PN and PH materials.

The fracture strength is practically independent of the molecular mass for the TPS materials. The molar mass dependence of the fracture strength is predominantly due to entanglements[24]. Beyond a critical molecular mass for entanglements, additional entanglements no longer contribute to the strength of the physical network created by the entanglements.

The maximal values of the elongation and the energy to break point are influenced by starch molecular mass. The maximal values of the strain at break in the rubbery state of the PN and PH materials are 100–125% and 30–50%, respectively. The values of the energy to break point at the maximum of the PN and PH materials are 0.15 ± 0.02 and $0.1 \pm 0.01\,J\,mm^{-2}$, respectively. This value is found at the glass-to-rubber transition at a water content of 9–10%. The differences in strain at break and energy to break point in the rubbery state (9–15% water) are explained by the differences in molecular mass of amylopectin and amylose of the PN and PH materials. In the rubbery state, the entangled polymers with a higher molecular mass can be stretched much further than polymers with a low molecular mass[24] and de-entanglement of the polymers is more difficult. This will also be reflected in a higher value for the total energy needed to break the materials (the tearing energy) in the rubbery state. The energy required to extend a rubber to its ultimate elongation is related to the length of the chain of the starch molecules and thus to molecular mass. For starch there is a complicating factor that amylose and amylopectin differ in degree of branching. There is no linear relationship between average molecular mass of starch and the chain length. For amylose and amylopectin the relationships of molecular mass with shape and size are dependent on the degree of branching. The TPS materials can be visualized as a matrix of entangled amylose and amylopectin molecules. This type of network formation is similar to that described for amylose and starch gelation[48]. For amylopectin only the short outer chains

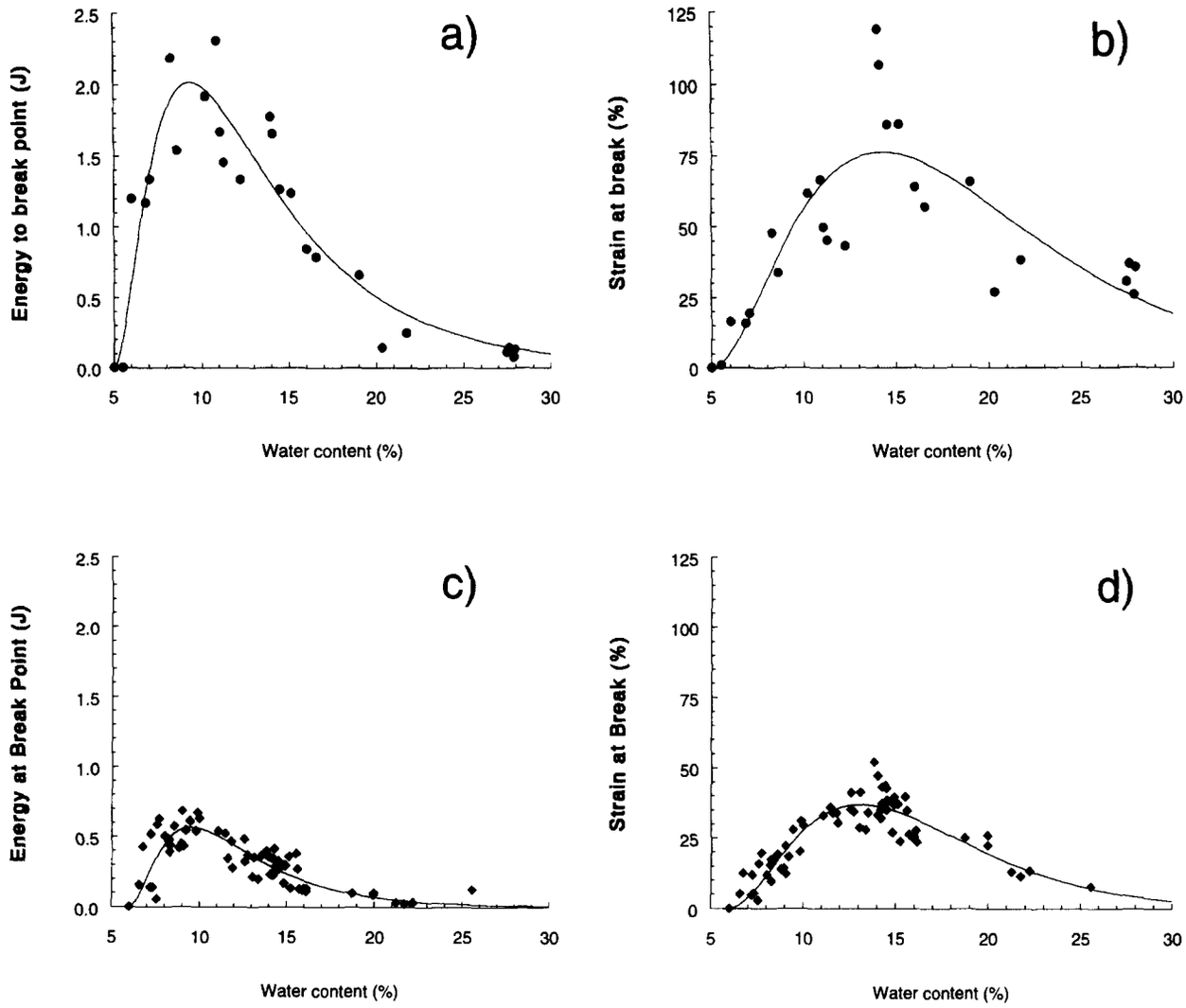

Figure 8 The strain at break (elongation) and tearing energy as a function of water content. ●, Elongation (a) and energy (b) of the PN TPS materials; ◆, elongation (c) and energy (d) of the PH TPS materials

of the amylopectin can participate in the formation of entangled structures with the outer chains of other amylopectin molecules or with amylose. The amount of amylose and the amylose chain length is lowered by acid hydrolysis. Hydrolysis of amylopectin has been shown (unpublished results) to affect the degree of branching of the amylopectin. Low molecular mass chains are chipped off from the outside thereby lowering the molecular mass and the degree of branching. Thus, a lowering of the molecular mass of amylose as well as amylopectin and of the degree of branching explain the differences in measured values of the elongation and tearing energy of TPS materials without influencing the glass transition temperature and the E-modulus. However, it still has to be investigated which of the molecular changes is the most dominating factor for explaining the observed differences in stress–strain properties.

CONCLUSIONS

Polymer chemical principles have been successfully applied to explain the mechanical behaviour of the TPS materials made from a high or from a low molecular mass starch. Both materials are viscoelastic with three characteristic regions of mechanical behaviour as a function of water content: a glassy region, a rubbery region preceded by a glass-to-rubber transition and a gel-like region. At high water content the materials are viscous, due to the low interaction forces and the reduced hydrogen bonding between the starch polymers in the amorphous regions. The materials are composed of a complex network of completely plasticized starch, recrystallized starch, partially destructurized granular starch and intact granular starch. Both amylose and amylopectin are responsible for the semicrystalline nature of the TPS materials.

Acid hydrolysis of potato starch reduces the chain length of amylose and the chain length and the degree of branching of amylopectin. These low molecular mass starches give TPS materials with a less effectively entangled matrix of amylose and amylopectin polymers. In the rubbery state, this results in a lowering of the elongation at break and tearing energy.

ACKNOWLEDGEMENTS

This work has been supported by the Netherlands Program for Innovation Oriented Carbohydrate Research (IOP-k) with financial aid of the Ministry of Economic Affairs and the Ministry of Agriculture,

Nature Management and Fisheries. The authors wish to thank Ursula Kroesen for her work on the influence of water content on the properties of TPS.

REFERENCES

1 *Plastic News* 1992, **4**, 27
2 Gonsalves, K. E., Patel, S. H. and Chen, X. *J. Appl. Polym. Sci.* 1991, **43**, 405
3 Gonsalves, K. E., Wong, T. K., Patel, S. H., Chen, X. and Trivedi, D. *Polym. Mater. Sci. Eng.* 1990, **63**, 854
4 Imam, S. H., Gould, J. M., Gordon, S. H., Kinney, M. P., Ramsey, A. M. and Tosteson, T. R. *Current Microbiol.* 1992, **25**, 1
5 Goheen, S. M. and Wool, R. P. *J. Appl. Polym. Sci.* 1991, **42**, 2691
6 Bastioli, C., Bellotti, V., Del Giudice, L. and Lombi, R. *PCT Int. Appl.* WO/9102024, 1991, 1
7 Stepto, R. F. T., Tomka, I. and Thoma, M. *Eur. Patent Appl.* EP 304401, 1989, 1
8 Bastioli, C., Bellotti, V., Del Tredici, G., Lombi, R., Montino, A. and Ponti, R. *PCT Int. Appl.* WO 9219680, 1992, 1
9 Röper, H. and Koch, H. *Starch* 1990, **42**, 123
10 Wiedmann, W. and Strobel, E. *Starch* 1991, **43**, 138
11 Chinnaswamy, R. and Hanna, M. A. *Starch* 1991, **43**, 396
12 Stepto, R. and Tomka, I. *Chimia* 1987, **41**, 76
13 Blanshard, J. M. V. in 'Starch, Properties and Potential' (Ed. T. Galliard), Wiley, New York, 1987, p. 16
14 Kugimiya, M. and Donovan, J. W. *J. Food Sci.* 1981, **46**, 765
15 Sievert, D. and Holm, J. *Starch* 1993, **45**, 136
16 Praznik, W. *Starch* 1986, **38**, 292
17 Klingler, R. W. and Zimbalski, M. *Starch* 1992, **44**, 414
18 Bader, H. G. and Göritz, D. *Starch* 1994, **46**, 435
19 Jane, J.-L. and Chen, J.-F. *Cereal Chem.* 1992, **69**, 60
20 Clark, A. H., Gidley, M. J., Richardson, R. K. and Ross-Murphy, S. B. *Macromolecules* 1989, **22**, 346
21 Whistler, R. L. and Hilbert, G. E. *Ind. Eng. Chem.* 1944, **36**, 796
22 Warburton, S. C., Donald, A. M. and Smith, A. C. *Carbohydrate Polym.* 1993, **21**, 17
23 Wolff, I. A., Davis, H. A., Cluskey, J. E., Gundrum, L. J. and Rist, C. E. *Ind. Eng. Chem.* 1951, **43**, 915
24 Elias, H.-G. in 'An Introduction to Plastics', VCH, Weinheim, 1993, p. 169
25 Zobel, Z. F. *Starch* 1988, **40**, 44
26 Zeleznak, K. J. and Hoseney, R. C. *Cereal Chem.* 1987, **64**, 121
27 Orford, P. D., Parker, R., Ring, S. G. and Smith, A. C. *Int. J. Biol. Macromol.* 1989, **11**, 91
28 Shogren, R. L., Swanson, C. L. and Thompson, A. R. *Starch* 1992, **44**, 335
29 Westhoff, R. P., Kwolek, W. F. and Otey, F. H. *Starch* 1979, **31**, 163
30 Protzman, T. F., Wagoner, J. A. and Young, A. H. U.S. Patent 3.344.216, 1967, 1
31 Wittwer, F. and Tomka, I. U.S. Patent 4.673.438, 1987, 1
32 Lay, L. S., Rehm, J., Stepto, R. F., Thoma, M., Sachetto, J. P., Lentz, D. J. and Silbiger, J. U.S. Patent 5.095.054, 1992, 1
33 Shogren, R. L., Swanson, C. L. and Thompson, A. R. *Starch* 1992, **44**, 335
34 Kirby, A. R., Clark, S. A., Parker, R. and Smith A. C. *J. Mater. Sci.* 1992, **28**, 5937
35 Ollett, A.-L., Parker, R. and Smith, A. C. *J. Mater. Sci.* 1991, **26**, 1351
36 Young, J. F. *J. Appl. Chem.* 1967, **17**, 241
37 Wyatt, P. J. in 'Laser Light Scattering in Biochemistry' (Eds S. E. Harding, D. B. Sattelle and V. A. Bloomfeld), Royal Society of Chemistry, Cambridge, 1992, p. 35
38 Banks, W., Geddes, R., Greenwood, C. T. and Jones, I. G. *Starch* 1972, **24**, 245
39 Cameron, D. G. and Moffat, D. J. *J. Test Eval.* 1984, **12**, 78
40 Hermans, P. H. and Weidinger, A. *J. Polym. Sci.* 1949, **4**, 135
41 Robin, J. P., Mercier, C., Charbonniere, R. and Guilbot, A. *Cereal Chem.* 1974, **51**, 389
42 Appelqvist, I. A. M., Cooke, D., Gidley, M. J. and Lane, S. J. *Carbohydrate Polym.* 1993, **20**, 291
43 Shogren, R. L. *Carbohydrate Polym.* 1992, **19**, 83
44 Orford, P. D., Parker, R. and Ring, S. G. *Int. J. Biol. Macromol.* 1989, **11**, 91
45 Soest, J. J. G. van, Wit, D. de., Tournois, H., Vliegenthart, J. F. G. *Carbohydrate Res.* 1995, **279**, 201
46 Lai, L. S. and Kokini, J. L. *Biotechnol. Prog.* 1991, **7**, 251
47 Soest, J. J. G. van, Wit, D. de., Tournois, H. and Vliegenthart, J. F. G. *Polymer* 1994, **35**, 4722
48 Morris, V. J. *Trends Food Sci. Technol.* 1990, **7**, 2